CrystEngComm

COMMUNICATION

View Article Online
View Journal | View Issue

Cite this: *CrystEngComm*, 2014, **16**, 10937

Received 4th September 2014,
Accepted 10th October 2014

DOI: 10.1039/c4ce01826e

www.rsc.org/crystengcomm

Environment friendly template-free microwave synthesis of submicron-sized hierarchical titania nanostructures and their application in photovoltaics†

Sofia Javed,* Muhammad Aftab Akram and Mohammad Mujahid

A simple low-temperature microwave synthesis of hierarchical nanostructures (HNSs) of titania in DI water is reported. A great advantage of the reported method is the production of submicron-sized HNSs without any surfactant or hydrofluoric acid. The hierarchical morphology provides huge surface area for maximum exposure for light-driven reactions, and the 3D folding morphology allows further scattering of light to obtain its maximum utilization. FESEM, TEM, XRD, BET surface area measurement, UV/VIS and Raman spectroscopy were utilized to understand the structures. The mechanism of formation of nanostructures is also discussed. The nanostructures were employed in dye-sensitized solar cells for performance comparison.

Titania nanostructures being thermally and chemically stable, cheap and nontoxic[1,2] offer their potential for use in various applications including photocatalysis,[3–5] photovoltaics,[6,7] gas sensors,[8,9] adsorbents, supports and many others.[10] Among various nanostructures of titania, the synthesis of nanoparticles/spheres,[6,11] nanobelts,[12] nanorods,[7,13] nanowires[14] and nanotubes[15] can be found in a number of reports in the literature, but relatively few reports on the synthesis of hierarchical nanostructures (or nanoflowers) of titania can be found.[9,14,16–19] The hierarchical morphology offers large specific surface area (enabling greater generation and migration of photocarriers from adsorbed species on the surface), light absorption improvement and high refractive index (enabling higher light absorption and refraction); hence, they offer high photocatalytic efficiency.[2] The reports on the synthesis of HNSs of titania include hydro/solvothermal synthesis, microemulsion synthesis, sol–gel method, hydrolysis/alkolysis and electrodeposition oxidation methods.[2,9,14,16–19] Generally, the synthesis of titania HNSs makes use of organic/inorganic salts of Ti, surfactants, highly toxic hydrofluoric acid, and high temperature and pressure. Most of the reported HNSs produced by the said methods have diameters in the micron range, except those produced by the microemulsion using surfactants and hydrolysis/alkolysis methods (producing smaller nanoflowers); however, these methods have issues of difficult control due to many parameters governing the process.[2] Microwave-synthesized nanostructures possess high specific surface area and good photocatalytic and redox properties.[20] The microwave synthesis of nano-titania with different architectures including nanoparticles,[4,21] nanotubes,[5,12,20] nanorods,[22,23] and nanospheres[23,24] has evolved as an instant, efficient and cheap fabrication route. There are a few reports on microwave synthesis of titania HNSs.[14,17] Rahal *et al.* have reported the microwave synthesis of titania nanoflowers using TiF_4, template CTAB and urea at a temperature of 120 °C in water, although they have not used hydrofluoric acid; however, the surface directing agent plays the main role in the formation of nanoflowers.[17] Huang *et al.* report the formation of titanate nanoflowers by microwave treatment of titania nanopowders in 8 M aqueous NaOH at 240 °C for 45 minutes.[14]

This report presents an instant economical method to produce HNSs at 1 atm and 100 °C in 5 minutes in 10 M NaOH aqueous solution. Submicron-sized HNSs of titania are prepared under environment friendly conditions with no hydrofluoric acid, organic additives and surfactants. Microwave treatment was applied to anatase powder dispersed in aqueous 10 M sodium hydroxide solution for different durations (5 to 20 minutes) at a power of 250 W.

Table 1 depicts the sample designation with different treatment times along with crystallite sizes calculated from XRD plots using the Scherrer equation, degree of crystallinity calculated using XRD peak areas, bandgap values measured using UV/VIS spectroscopy[25] (ESI†) and BET surface area values for different samples. Fig. 1 shows a plot for crystallite size, bandgap and surface area with increasing microwave exposure. Although the anatase phase of titania has a bandgap of 3.2 eV, the high bandgap values obtained here

School of Chemical and Materials Engineering, National University of Sciences and Technology, H-12, Islamabad, Pakistan. E-mail: sofiajaved@scme.nust.edu.pk

† Electronic supplementary information (ESI) available. See DOI: 10.1039/c4ce01826e

Table 1 Crystallite size, degree of crystallinity, bandgap and BET surface area values for different samples treated with microwave radiation for different durations

Sr. no.	Sample ID	Treatment duration (minutes)	Crystallite size (nm) (XRD)	Degree of crystallinity	Bandgap (eV)	BET surface area (m^2 g^{-1})
1	T1	0	5.6	0.85	3.83	191
2	MT2	5	7.2	0.62	3.75	82
3	MT3	10	10.1	0.79	3.7	68
4	MT4	15	13.0	0.79	3.67	25
5	MT5	20	13.8	0.66		18

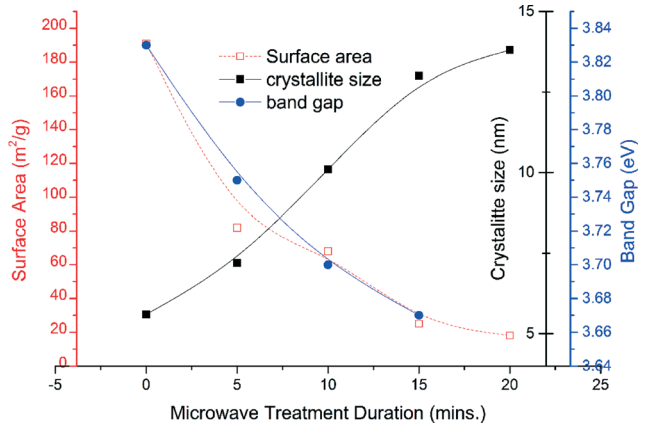

Fig. 1 Variation of bandgap, crystallite size and surface area with microwave treatment duration of 0, 5, 10, 15 and 20 minutes.

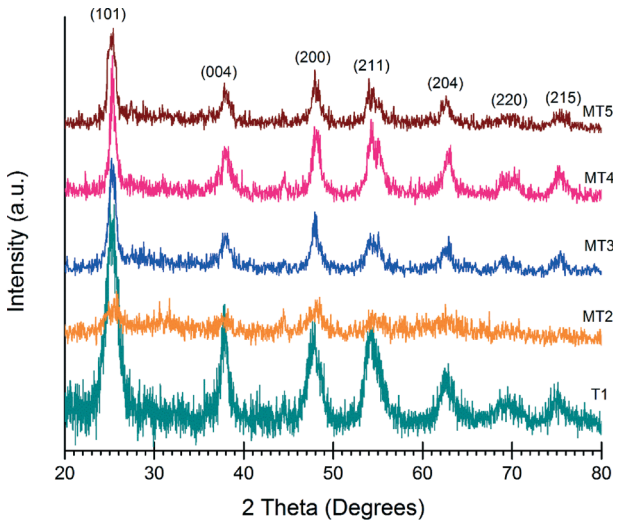

Fig. 2 XRD plots of starting material T1 and microwave-treated samples MT2 (5 min), MT3 (10 min), MT4 (15 min) and MT5 (20 min) after annealing at 450 °C for 1 hour.

for all of the samples can be attributed to the small crystallite size of the starting material.[26] The bandgap and the surface area decrease as the microwave treatment time increases, and the crystallite size increases with an increase in microwave exposure time.

As stated earlier, the starting material is the anatase phase of titania. The titania quantum dots with crystallite sizes of around 5 nm were prepared by the sol–gel reflux synthesis described in our previous report.[11] The small crystallite size has resulted in the formation of small HNSs (nanoflowers) in all of the samples after microwave treatment without the use of any surfactant. The small HNSs are advantageous for offering huge surface area and retaining the light trapping effects for better efficiency in photocatalytic devices.

The XRD plots as shown in Fig. 2 reveal that the anatase phase is the major crystalline phase in all of the samples with different microwave treatment durations. All peaks match with those of the tetragonal anatase phase with space group *I*41/*amd* and are indexed (reference code: 01-071-1168).

FESEM images of the starting material and the treated samples are shown in Fig. 3. Titania HNSs of sizes around 500 nm can be observed. With the increase in the microwave treatment from 5 to 20 minutes, the morphology is gradually becoming sharper with little or no effect on the sizes of the HNSs.

Fig. 4 shows the TEM images of MT2 and MT4. Here, we can observe that the HNSs are made up of somewhat radially arranged nanosheets. With the increase in the treatment time, the nanosheets have twisted and rolled along their sides. This can be related to the formation mechanism of nanotubes with the same contents under hydrothermal conditions.[27] It should be mentioned here that although the synthesis conditions are similar to the formation of nanotubes under hydrothermal treatment, the HNSs are stable as the results shown in this report are all obtained after annealing of the treated samples at 450 °C for 1 hour. The formation mechanism of these HNSs will be discussed later. From TEM, the crystallite size is not quantifiable. The crystallite size calculated from XRD plots using the Scherrer equation may be called the effective crystallite size of the corresponding samples.

Fig. 5 shows the Raman spectra of the samples. They have peaks corresponding to the anatase phase of titania. The anatase phase of titania is found with the following Raman modes: three Eg modes at 169 (Eg (1)), 196 and 641 cm^{-1} and two B1g modes at 397 and 518 cm^{-1}. The A1g mode at 513 cm^{-1} seems to be embedded in the peak at 518 cm^{-1}.[28] The variations in the Raman intensity can be related to the variations in the surface roughness of the starting material and those after microwave treatment. The starting sample has ~5 nm crystallites with ~20 nm particles and shows a maximum intensity among the Raman spectra as the small crystallite size gives large shift and broadening of the Raman band.[29] After microwave treatment, the surface roughness gradually increases from 5 to 20 minute treatment duration and the Raman intensity also increases with the increase in

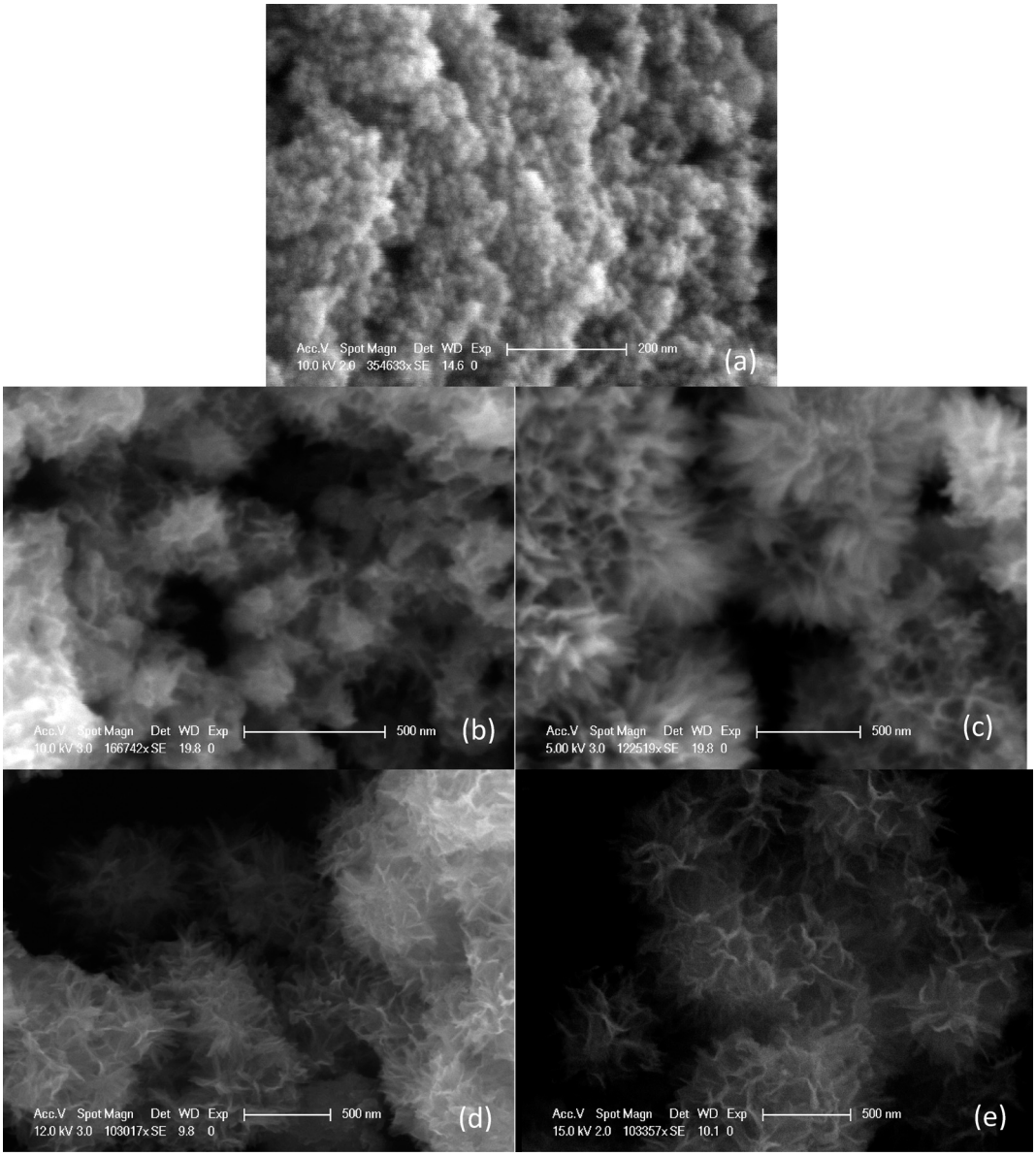

Fig. 3 FESEM images of titania nanostructures T1 (a), MT2 (b), MT3 (c), MT4 (d), and MT5 (e).

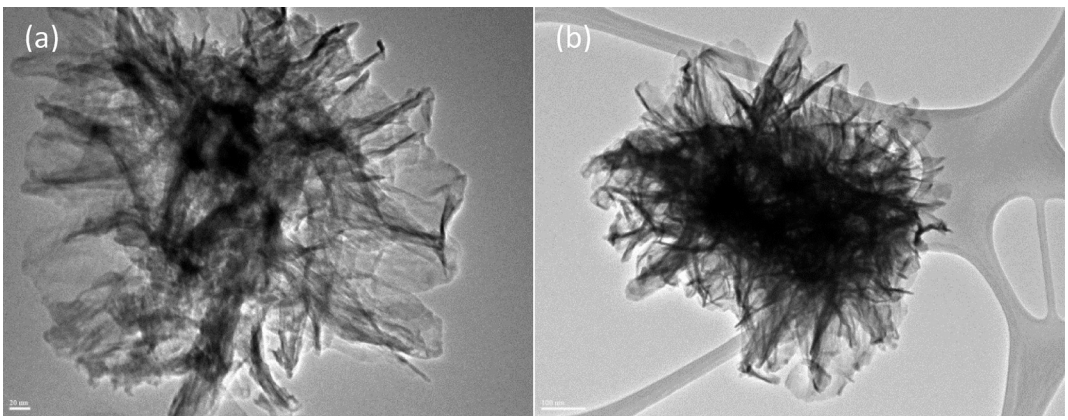

Fig. 4 TEM images of hierarchical nanostructures of titania MT2 (a) and MT5 (b).

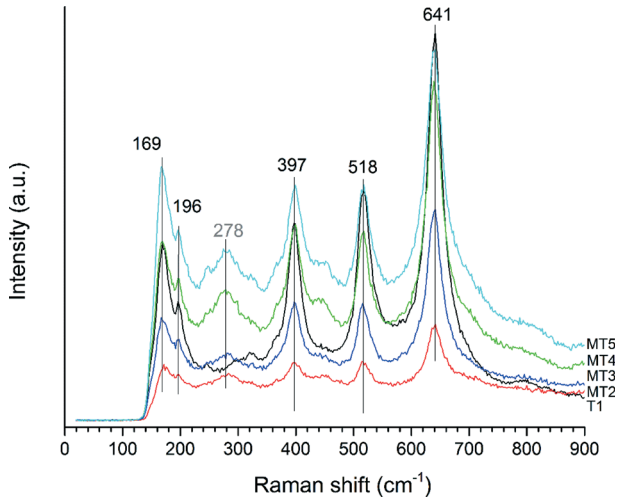

Fig. 5 Raman spectra of titania HNSs MT2, MT3, MT4, and MT5 and the starting nanopowder T1.

treatment duration due to formation of distinct few nanometer thick sheets of the HNSs.

The growth mechanism may be related to the reported mechanism for the formation of titania nanotubes under hydrothermal conditions using titania nanoparticles in 10 M NaOH solution, *i.e.* on dissolution of the starting titania nanoparticles under highly alkaline medium and under hydrothermal atmosphere, nanosheets are formed which afterwards roll over to make titania nanotubes.[27] In the present case, the situation is somewhat different in that small duration exposure to microwaves is provided for the same contents at atmospheric pressure. In this situation, it is speculated that the surface of the starting titania nanoparticles begins to dissolve. Subsequently, regrowth occurs on the particles in the form of sheets giving rise to hierarchical morphology.

The increase in crystallite size and consequent decrease in surface area and bandgap values upon evolution of the HNSs with increasing microwave exposure are justified. The crystallinity[25] values are calculated using XRD peak areas and are given in Table 1. It is indicated that the crystallinity decreases after 5 minute microwave exposure owing to more dissolution than regrowth. Then, it increases till 15 minutes treatment due to increased regrowth of the sheets in the HNSs. On 20 minutes exposure, although the crystallite size has increased, the decrease in crystallinity can be explained by considering random orientation of the planes in the rolling sheets of HNSs, with respect to the incident X-rays. We can see from SEM that the morphology of the HNSs seems to be going to the depth on increasing the microwave treatment duration from 5 to 20 minutes. Also, the TEM images can reveal that the MT2 sample seems to have some unchanged central zone, while for the MT5 sample, the conversion seems to be nearly completed. A schematic illustrating the speculated growth mechanism is given in Fig. 6.

It should be mentioned that under the microwave treatment of titania nanoparticles, the 3D morphology is thought

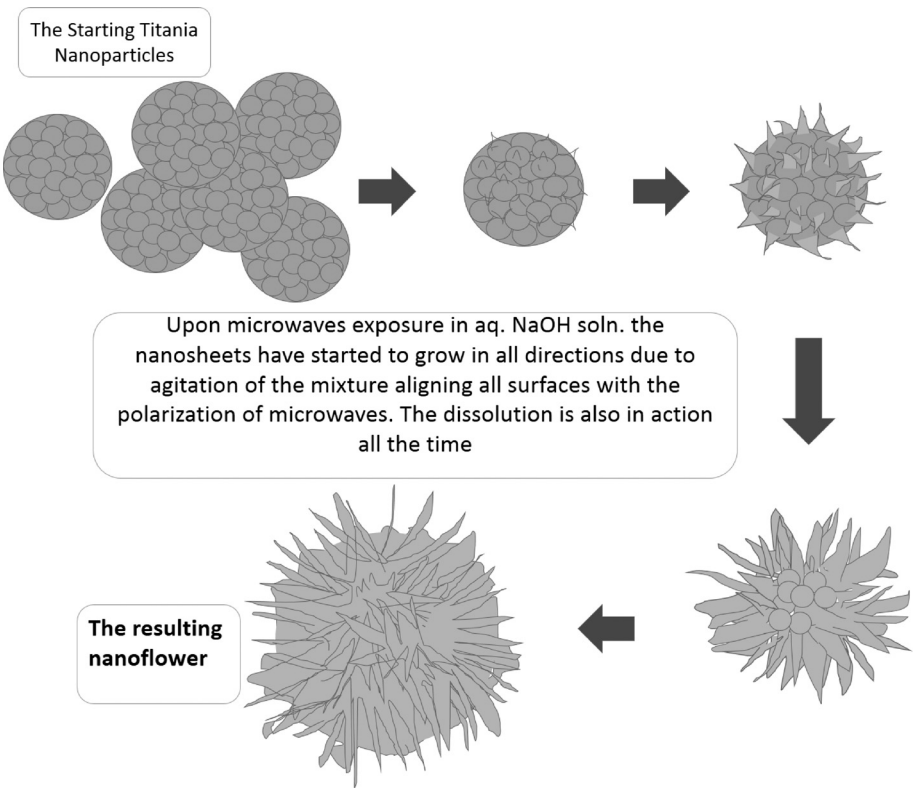

Fig. 6 Schematic for the growth mechanism of titania HNSs.

to be the result of a role played by microwaves specifically. Titania particles start to dissolve, and due to polarization effects of the radiation, they regrow three-dimensionally in the form of sheets giving nanoflower-like structures. With the increase in the treatment duration, the depth of the twisted nanosheets seems to be increased due to more and more dissolution of the starting material and growth of the sheets as evident from the TEM images (Fig. 4).

In order to check the role of microwaves, an experiment with reflux condensation at 100 °C was carried out for the same contents but outside the microwave oven for a duration of 20 minutes. In another experiment, titania powder in 10 M NaOH was heated in a sealed vessel at 100 °C for 20 minutes, *i.e.* under hydrothermal conditions. The treated powders were washed several times with DI water and annealed at 450 °C for 1 hour. HNSs were not formed in both of these experiments (ESI†). This reveals that microwave treatment under atmospheric pressure is playing the main role in producing HNSs without using any template and hazardous chemicals like HF or H_2O_2.

All the microwave reactions were carried out in a domestic oven under refluxing using the assembly shown in the schematic (Fig. 7). The commercial microwave reactor cannot be used for highly alkaline media due to exploding hazard of the sealed pressurized reactor vessel.

The HNSs were employed in DSSCs in comparison with the starting material T1. FTO-coated glass slides were cleaned, and a blocking layer of titania was fabricated by spin coating a 2% solution of titanium tetraisopropoxide in isopropanol. Pastes of the synthesized titania powders and T1 were made and films were fabricated by the doctor blade method. A monolayer of N719 dye was infused on titania films by overnight soaking of the titania-coated FTO glass slides in the dye solution. Pt counterelectrodes were used. Liquid iodide/triiodide electrode was filled in between the two electrodes. *JV* measurement was obtained under 1 sun illumination. Fig. 8 shows the *JV* curves for the DSSCs having

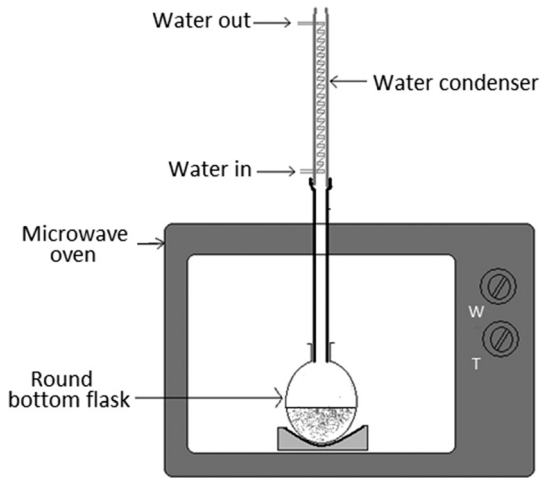

Fig. 7 Schematic illustrating the experimental setup for microwave treatment of different samples.

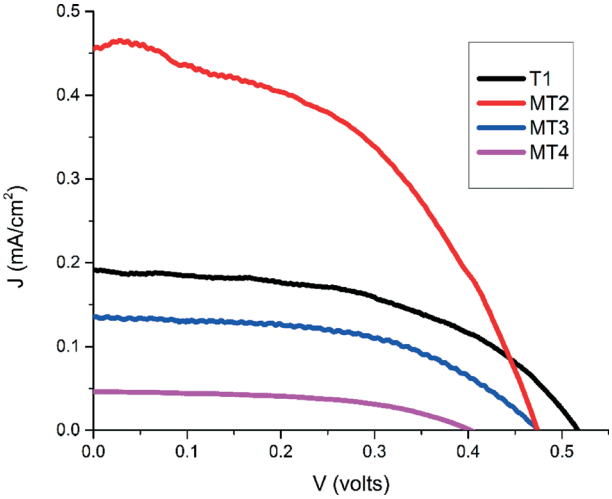

Fig. 8 *JV* curves for DSSCs employing T1, MT2, MT3 and MT4 as the semiconductor layer.

Table 2 Photovoltaic parameters determined from *JV* curves of DSSCs employing synthesized hierarchical nanostructures and starting titania

Sr. no.	Sample	ff	V_{oc} (volts)	J_{sc} (mA cm^{-2})	η (%)
1	T1	0.49	0.5174	0.1915	0.0489
2	MT2	0.48	0.4739	0.4647	0.1055
3	MT3	0.53	0.4748	0.1356	0.03395
4	MT4	0.51	0.4036	0.0461	0.00955

T1, MT2, MT3 and MT4 as the semiconductor layer. Table 2 gives the fill factor, open circuit voltage, short circuit current density and efficiency values for the devices. Maximum efficiency of 0.1% is achieved with the sample MT2, *i.e.* HNSs produced after 5 minute microwave exposure.

The open circuit voltage is maximum for the device with T1, is decreasing for MT2 and MT3 and is minimum for MT4. This decrease can be explained considering the decrease in bandgap of the samples with increasing microwave exposure. V_{oc} for DSSCs is dependent on the difference between the redox potential of the electrolyte and the conduction band of titania.[30] With the decrease in bandgap of titania powders, the conduction band seems to be lowered resulting in the decrease in V_{oc} in DSSCs. The current density is exhibiting an increase with evolution of hierarchical morphology upon microwave treatment. But as the surface area is also decreasing with increased microwave exposure, the net current density is decreased after 5 minutes. The sample MT2 has reasonably high surface area, *i.e.* 82 m^2 g^{-1} (Table 1), with a morphology that is a mix of nanoparticles contributing to the surface area and radially arranged nanosheets for greater light absorption giving a maximum current density among all of the samples. Samples MT3 and MT4 have low surface areas of 24 and 18 m^2 g^{-1} (Table 1), thus showing low current densities in DSSCs. These samples may perform better when used in combination with nanoparticles to combine the light scattering effects of hierarchical morphology and huge surface area of the nanoparticles.

Conclusion

We have presented an environment friendly instant microwave method of making hierarchical nanostructures of titania with sizes less than 1 micron. HNSs are produced by the microwave treatment of titania (anatase) powder in 10 M NaOH aqueous solution at 1 atm and 100 °C for small durations ranging from 5 to 20 minutes. The specialty of this report is to present a method of making titania HNSs without using hazardous chemicals and high temperature and pressure. XRD, FESEM, TEM and Raman spectroscopy are utilized for understanding the structures. These submicron titania hierarchical nanoflowers are then employed in DSSCs for performance comparison with the starting material. The sample after 5 minute microwave treatment having a surface area of 82 $m^2 g^{-1}$, a mixture of nanoparticles and hierarchical morphology shows maximum efficiency of 0.1%. The samples with longer microwave treatment have relatively low surface areas due to conversion to hierarchical morphology and hence are unable to give better performance when used alone. A mix of nanoparticles and the hierarchical nanostructures is beneficial for scattering and thus greater absorption of light with large surface area for better performance of the DSSCs.

Acknowledgements

The authors are grateful to the Centre of Super Diamond and Advanced Films (COSDAF), City University of Hong Kong for facilitating characterization.

References

1 V. Gomez, A. M. Balu, J. C. Serrano-Ruiz, S. Irusta, D. D. Dionysiou, R. Luque and J. Santamaria, *Appl. Catal., A*, 2012, **441**, 47–53.
2 Z. Wu, Q. Wu, L. Du, C. Jiang and L. Piao, *Particuology*, 2014, **15**, 61–70.
3 D. Kong, J. Z. Y. Tan, F. Yang, J. Zeng and X. Zhang, *Appl. Surf. Sci.*, 2013, **277**, 105–110.
4 S. Sitthisang, S. Komarneni, J. Tantirungrotechai, Y. Dong Noh, H. Li, S. Yin, T. Sato and H. Katsuki, *Ceram. Int.*, 2012, **38**, 6099–6105.
5 Y. P. Peng, S. L. Lo, H. H. Ou and S. W. Lai, *J. Hazard. Mater.*, 2010, **183**, 754–758.
6 C.-Y. Liao, S.-T. Wang, F.-C. Chang, H. P. Wang and H.-P. Lin, *J. Phys. Chem. Solids*, 2014, **75**, 38–41.
7 M. Zhu, L. Chen, H. Gong, M. Zi and B. Cao, *Ceram. Int.*, 2014, **40**, 2337–2342.
8 S. Park, S. An, H. Ko, S. Lee, H. W. Kim and C. Lee, *Appl. Phys. A*, 2013, **115**, 1223–1229.
9 C. Wang, L. Yin, L. Zhang, Y. Qi, N. Lun and N. Liu, *Langmuir*, 2010, **26**, 12841–12848.
10 B. Choudhury and A. Choudhury, *Mater. Sci. Eng., B*, 2013, **178**, 794–800.
11 S. Javed, M. Mujahid, M. Islam and U. Manzoor, *Mater. Chem. Phys.*, 2012, **132**, 509–514.
12 S. Ribbens, V. Meynen, G. V. Tendeloo, X. Ke, M. Mertens, B. U. W. Maes, P. Cool and E. F. Vansant, *Microporous Mesoporous Mater.*, 2008, **114**, 401–409.
13 L. Meng, C. Li and M. P. Santos, *J. Inorg. Organomet. Polym. Mater.*, 2013, **23**, 787–792.
14 J. Huang, Y. Cao, Z. Liu, Z. Deng and W. Wang, *Chem. Eng. J.*, 2012, **191**, 38–44.
15 G. H. Du, Q. Chen, R. C. Che, Z. Y. Yuan and L. M. Peng, *Appl. Phys. Lett.*, 2001, **79**, 3702–3704.
16 S. H. Ahn, D. J. Kim, W. S. Chi and J. H. Kim, *Adv. Mater.*, 2013, **25**, 4893–4897.
17 R. Rahal, A. Wankhade, D. Cha, A. Fihri, S. Ould-Chikh, U. Patil and V. Polshettiwar, *RSC Adv.*, 2012, **2**, 7048.
18 S. S. Mali, C. A. Betty, P. N. Bhosale, R. S. Devan, Y.-R. Ma, S. S. Kolekar and P. S. Patil, *CrystEngComm*, 2012, **14**, 1920.
19 S. S. Mali, C. A. Betty, P. N. Bhosale and P. S. Patil, *CrystEngComm*, 2011, **13**, 6349.
20 Y. C. Chen, S. L. Lo and J. Kuo, *Water Res.*, 2011, **45**, 4131–4140.
21 Y.-C. Wu and Y.-C. Tai, *J. Nanopart. Res.*, 2013, **15**, 1–11.
22 V. Rodríguez-González, S. Obregón-Alfaro, L. M. Lozano-Sánchez and S.-W. Lee, *J. Mol. Catal. A: Chem.*, 2012, **353–354**, 163–170.
23 T. Suprabha, H. G. Roy, J. Thomas, K. Praveen Kumar and S. Mathew, *Nanoscale Res. Lett.*, 2008, **4**, 144–152.
24 S. Yoon, E. S. Lee and A. Manthiram, *Inorg. Chem.*, 2012, **51**, 3505–3512.
25 R. J. Tayade, R. G. Kulkarni and R. V. Jasra, *Ind. Eng. Chem. Res.*, 2006, **45**, 922–927.
26 N. Sakai, Y. Ebina, K. Takada and T. Sasaki, *J. Am. Chem. Soc.*, 2004, **126**, 5851–5858.
27 H. Ou and S. Lo, *Sep. Purif. Technol.*, 2007, **58**, 179–191.
28 X. Chen and S. S. Mao, *Chem. Rev.*, 2007, **107**, 2891–2959.
29 J. Bandet, J. Frandon, F. Fabre and B. D. Mauduit, *Jpn. J. Appl. Phys.*, 1993, **32**, 1518–1522.
30 M. Gratzel, in *Solar Energy*, ed. C. L. Richter, D. Gueymard and A. Christian, Springer, New York, 2013, vol. XV, p. 744.

